Acta Geod Geophys (2017) 52:283–299
DOI 10.1007/s40328-016-0182-4

ORIGINAL STUDY

Improvement of seismic structural interpretation of Zagros fold-thrust belt by dip scanning in common diffraction surface imaging method

Mehrdad Soleimani[1] · Behshad Jodeiri Shokri[2] · Mehrnoush Rafiei[3]

Received: 27 July 2015 / Accepted: 3 August 2016 / Published online: 13 August 2016

Abstract Geological interpretation and seismic imaging on data acquired from complex media, especially when accompanied by a thick layer of salt and/or anhydrate, is always a controversial task. The aim of this study is to introduce a method for seismic imaging of complex structures and study the folding scenario of the Zagros overthrust in SW Iran based on the improved seismic image processed by the proposed method. A diffraction based version of the common reflection surface stack method, called the common diffraction surface (CDS), was selected to enhance quality of seismic image from the Zagros fold-thrust belt. The 2D CDS method was also developed here to 3D partial CDS. Consequently, three sets of 2D and a set of 3D seismic data were processed with the conventional Kirchhoff prestack time migration and the partial common diffraction surface methods. Geological models released in previous studies of the Zagros overthrust were used as the base model of interpretation. Structural interpretation on seismic sections with new method was in accordance with previous geological models and improved in some parts where the new method could enhance quality of the seismic image. Seismic structural interpretation shows the inner part of the belt was subjected to folding, uplift and erosion. This mechanism constituted a resistant mass in the Dezful Embayment in front of the SW moving thrust and folds. This resistant mass formed tightly folded or thrusted and highly shortened structures in the Izeh zone and High Zagros area. In the oil rich zone of the Dezful Embayment, the thick evaporate—rich Gachsaran Formation, decouples the folding

✉ Behshad Jodeiri Shokri
b.jodeiri@hut.ac.ir; behshad.jodeiri@gmail.com

Mehrdad Soleimani
msoleimani@shahroodut.ac.ir

Mehrnoush Rafiei
mehrnoush.rafiei@gmail.com

[1] Faculty of Mining, Petroleum and Geophysics, Shahrood University of Technology, Shahrood, Iran

[2] Department of Mining Engineering, Hamedan University of Technology, Hamedan, Iran

[3] School of Geology, College of Science, University of Tehran, Tehran, Iran

above it from the folding below, making seismic imaging of potential traps beneath the detachment horizons extremely difficult.

Keywords CRS method · Partial 3D CDS method · Seismic imaging · Zagros fold-thrust belt · Dezful Embayment

1 Introduction

Complex geometry in folding systems with highly dipping layers and thrust faults complicate simulation of seismic wave propagation in such media.

Besides complexity of simulating wave propagation in that media, different studies proved that strong velocity contrast of some geological units (like salt and anhydrate) with surrounding media is another great challenge for most of the seismic imaging algorithms and interoperation techniques (Albertin et al. 2001; Ray et al. 2004; Seitchick et al. 2009). Examples of such settings are Gulf of Mexico, Avon canyon in Benin (Dahomey) basin (Olabode and Adekoya 2008), Jeffara basin in southeastern Tunisia (Gabtni et al. 2012) and Qiangtang terrane, Tibetan plateau (Lu et al. 2009).

Complexity of seismic imaging and interpretation in those mentioned examples could be resolve by integrating various techniques to obtain high quality seismic image. Different methods could also be used for increasing signal to noise ratio and/or improve structural interpretation in such complex geological basins. Wang et al. (2014) used a new method for removing body waves and ambient noise from seismic data of such regions. Xu et al. (2014) used 3D seismic attributes for structural interpretation for Sichuan Basin in China. Pu et al. (2014) also used a specialized 3D seismic interpretation technique for Growth conditions and 3D seismic delineation of carboniferous barrier reefs in the southwestern Tarim basin in northwest China.

Seismic modeling also has been extensively used to plan accurate seismic acquisition surveys over complex salt related structures (Gjøystdal et al. 2007) and to improve seismic processing flows for processing related data (Raef 2009; Huang et al. 2010). However, in such media, due to seismic velocity heterogeneity and structural complexity, seismic rays are bent and produce non-hyperbolic arrival times in addition to the hyperbolic ones (Höcht et al. 1999) which make it difficult for defining morphology of the subsurface structures (Pu et al. 2009). In all of the cases mentioned above, the major problem was obtaining accurate and high quality seismic image for further structural interpretation, the problem that is going to be resolved here for the Zagros over-thrust by introducing dip scanning in common diffraction surface imaging method.

2 The Zagros over-thrust

The Zagros fold-and-thrust belt (ZFTB) is a NW–SE trending orogenic belt, which extends over about 2000 km from Turkey through NE Iraq and passes SW Iran down to the Strait of Hormuz (Fig. 1). Structural investigation performed by Berberian and King (1981), Sherkati et al. (2006) and Burberry et al. (2010), based on morphology of structures, the ZFTB was divided into two adjacent belts: the High Zagros Belt (HZB) and the Zagros Simply Folded Belt (ZSFB) separated by the High Zagros Fault (HZF) (Fig. 2a). Some

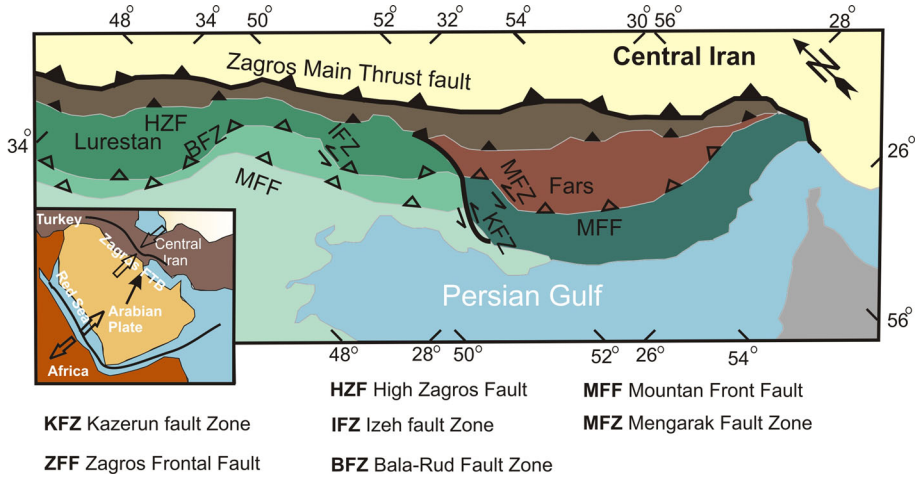

Fig. 1 Topographic relief and structural map, highlighting the overall geometry of the Iranian sector of the Zagros fold-thrust belt and the location of the major fault zones (modified after Sepehr et al. 2006)

cross sections from the ZFTB (location of profiles are defined in Fig. 2a) are shown in Fig. 2c. On the basis of lateral litho-facies variations, the Iranian part of the ZSFB was also divided into four different tectono-stratigraphic domains: The Fars province or eastern Zagros, the Izeh zone, the Dezful Embayment and finally the Lurestan province (Fig. 2a) (Sherkati et al. 2006). Stratigraphic column of the mentioned zones is shown in Fig. 2b. Based on the available data from Sherkati and Letouzey (2004) and Sepehr and Cosgrove (2004), deformation system of the Izeh fault and other zones of the ZFTB could be proved or further improved by detail seismic image structural interpretation integrated by the geological field observation.

However, low quality seismic image obtained from ZFTB suffers from two: acquisition obstacles and seismic data processing problems (Sepehr and Cosgrove 2004). As Tamimi et al. (2009) showed in their study, the main acquisition and data processing problem is poor illumination and accurate estimation of seismic velocity under incompetent units with plastic character (e.g. salt, shale and anhydrate). Sherkati et al. (2005) demonstrated that the position of such intermediate incompetent layer is an important factor controlling both structural style and fold wavelength.

In order to study variation and evolution of the ZFTB system in this study, newly introduced seismic imaging and interpretation techniques have been applied on some seismic data from this region. Four data sets from three different zones of the Zagros area were selected for further processing and interpretation here. Rectangles in Fig. 3, shows locations of the selected study areas.

3 Seismic imaging in complex structures

Structural interpretation on poor quality seismic image obtained from complex geological settings is a controversial task in the field of seismic interpretation (Pu et al. 2012). However, powerful depth seismic imaging methods could be applied to resolve some of possible obstacles in imaging of seismic data from those regions. Depth seismic imaging

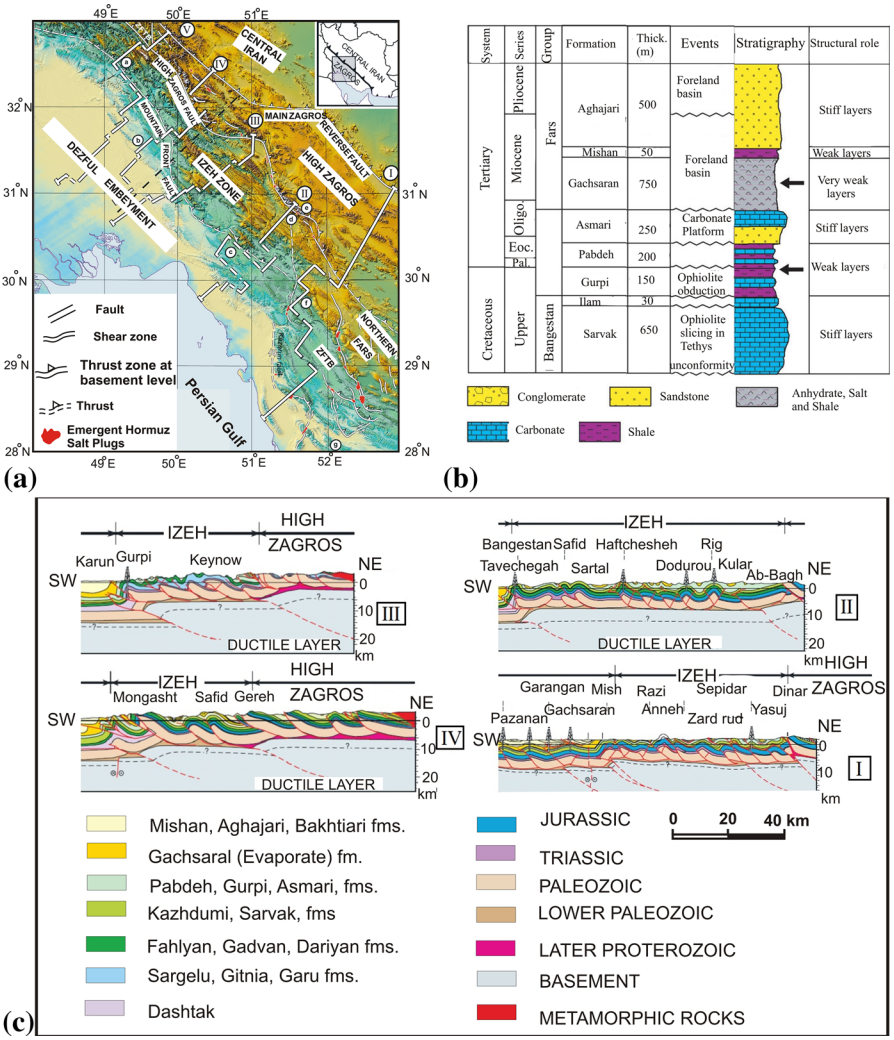

Fig. 2 **a** The Zagros fold thrust belt and its different parts. **b** The litho-stratigraphy column of the Zagros area and **c** different sections along the Zagros divided zones (Sherkati et al. 2006)

consists of two major closely linked steps, velocity estimation and migration (Fomel 2007). Biondi (2006) mentioned that a combination of velocity model building and migration is the key to successful imaging in such media. The full waveform inversion (FWI), reverse time migration (RTM) (Robein 2010), multi-focusing (Gelchinsky et al. 1999), common reflection surface (CRS) (Müller 1999; Mann 2002), partial common reflection surface stack (Baykulov and Gajewski 2009) and data based common diffraction surface (CDS) stack method (Soleimani et al. 2009) are some of the imaging methods used for complex media.

By using three kinematic wavefield attributes, the CRS stack method would considers the location, local orientation and curvature of the reflector in subsurface for seismic imaging (Mann 2002). Equation of the 2D CRS operator is as follows (Jäger 1999):

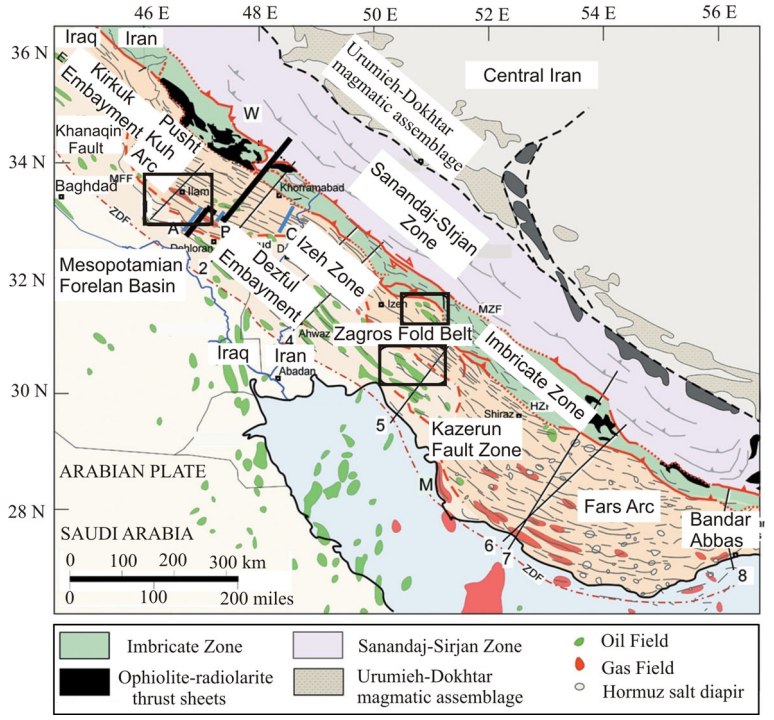

Fig. 3 Distribution of the oil and gas field in the Zagros overthrust, its zonation and location of the study area used for processing and interpretation that are defined by rectangles (Verges et al. 2011)

$$t_{\mathrm{hyp}}^2(x_m,h)=\left[t_0+\frac{2\sin\alpha(x_m-x_0)}{v_0}\right]^2+\frac{2t_0\cos^2\alpha}{v_0}\left[\frac{(x_m-x_0)^2}{R_{\mathrm{N}}}+\frac{h^2}{R_{\mathrm{NIP}}}\right] \quad (1)$$

where α is the emergence angle of normal ray at x_0, R_N is the wavefront curvature of hypothetic Normal wave and R_{NIP} is the wavefront curvatures of hypothetic NIP wave. Although the CRS stack method aims to enhance reflection events, this technique can also be adapted to enhance diffractions. Garabito et al. (2009) adapted the CRS stack approach for a situation where reflector shrinks to a diffraction point. Mann et al. (1999) previously mentioned that to simulate a hypothetic diffraction source on the reflector, the initial curvature of the wavefront starting at the source (R_N) should be zero. It requires that R_N be equal to R_{NIP} in the source point. To better explain diffraction enhancement operator, radius of this wavefront is called $R_{CDS} = R_{NIP} = R_N$. Thus equation of the 2D CDS method would be (Soleimani and Mann 2008):

$$t_{\mathrm{hyp}}^2(x_m,h)=\left[t_0+\frac{2\sin\alpha(x_m-x_0)}{v_0}\right]^2+\frac{2t_0\cos^2\alpha}{v_0R_{\mathrm{CDS}}}\left[(x_m-x_0)^2+h^2\right] \quad (2)$$

The idea of the partial CRS stack (Baykulov 2009) method was used in this study to modify the CDS stack equation. Müller (2003) developed the conventional 2D CRS to 3D by introducing eight kinematic wavefield attributes:

$$t_{hyp}^2 = \left(t_0 - \frac{2}{v}\mathbf{wm}\right)^2 + \frac{2t_0}{v}\left(\mathbf{m}^T\mathbf{Q}_{zyz}\mathbf{N}_N\mathbf{Q}_{xyz}^T\mathbf{m} + \mathbf{h}^\mathbf{T}\mathbf{P}_{zyz}\mathbf{N}_{NIP}\mathbf{P}_{zyz}^T\mathbf{h}\right) \quad (3)$$

where related to the local (x, y) system, centered at point $X_0(x_0,y_0)$, t_{hyp} describes the 3D hyperbolic traveltime approximation, t_0 is the two-way ZO traveltime at point $P_0(x_0, y_0, t_0)$, v is the surface velocity, **W** is the projection of the unit vector of the emerging normal ray at the ground surface. It contains the parameters (ψ,θ), *i.e.* angles that determine direction of propagation of two hypothetical wavefronts, NIP wave and N wave, along the emerging central (normal) ray. The NIP wave is associated with a point source exploding at the NIP. The Normal (N) wave relates to the "exploding reflector experiment". N_{NIP}, N_N are the 2×2 curvature matrices associated to the NIP and N-waves:

$$\mathbf{N}_i = \begin{pmatrix} \frac{1}{R_{i,\max}} & 0 \\ 0 & \frac{1}{R_{i,\min}} \end{pmatrix} \quad (4)$$

P, **Q** and **D** are given by:

$$\mathbf{P_{xyz}} = \mathbf{D_z}(\psi)\cdot\mathbf{D_y}(\theta)\cdot\mathbf{D_z}(\gamma_{NIP}), \quad \mathbf{Q_{xyz}} = \mathbf{D_z}(\psi)\cdot\mathbf{D_y}(\theta)\cdot\mathbf{D_z}(\gamma_N), \quad (5)$$

$$\mathbf{D_z}(\lambda) = \begin{pmatrix} \cos\lambda & \sin\lambda \\ \sin\lambda & \cos\lambda \end{pmatrix}, \quad \lambda = \psi, \gamma_{NIP}, \gamma_N \quad \mathbf{D_y}(\theta) = \begin{pmatrix} \cos\theta & 0 \\ 0 & 1 \end{pmatrix} \quad (6)$$

According to Eqs. (4), (5), and (6) the final eight search parameters are: ψ, θ, γ_{NIP}, γ_N, $R_{NIP,max}$, $R_{NIP,min}$, $R_{N,max}$ and $R_{N,min}$. To have advantage of the partial 2D CDS stack, the 2D partial CRS method of Baykulov (2009) and the conventional 3D CRS stack method of Müller (2003) were combined and improved here to 3D CDS stack, but into a partial form. Thus like as the 2D partial CDS stack, the 3D CRS equation should be modified to consider all the diffraction events.

Hence, radius of the normal wave and the NIP wave should coincide, too. Therefore, eight parameters are reduced to five parameters while: γ_{NIP}, $= \gamma_N$, $R_{NIP,max} = R_{N,max}$ and $R_{NIP,min} = R_{N,min}$. Finally these five parameters are: ψ, θ, γ_{CDS}, $R_{CDS,max}$, and $R_{CDS,min}$. The partial 3D CDS stack equation would be:

$$t_{hyp}^2 = \left(t_0 - \frac{2}{v}\mathbf{wm}\right)^2 + \frac{2t_0}{v}\left(\mathbf{m}^T\mathbf{Q}_{zyz}\mathbf{N}_{CDS}\mathbf{Q}_{xyz}^T\mathbf{m} + \mathbf{h}^\mathbf{T}\mathbf{P}_{zyz}\mathbf{N}_{CDS}\mathbf{P}_{zyz}^T\mathbf{h}\right) \quad (7)$$

4 The Pazanan area 2D seismic structural interpretation

The south western part of the ZFTB is a trapezoidal area covering 75,000 km^2 called the Dezful Embayment (Fig. 2a) (Sherkati et al. 2006; Alen and Talebian 2011). Activity of several low angle major thrust faults cutting, through nappes in this area, complicated structures of the Dezful Embayment (Letouzey et al. 2002; Alaei 2005). In order to study the lateral variations of structural geometry in the southeast of the Dezful Embayment, a seismic data from this region were used for further imaging and structural interpretation. Figure 4, shows obtained seismic sections from the seismic processed data with the conventional prestack time migration (PSTM) by the Kirchoff algorithm and the partial

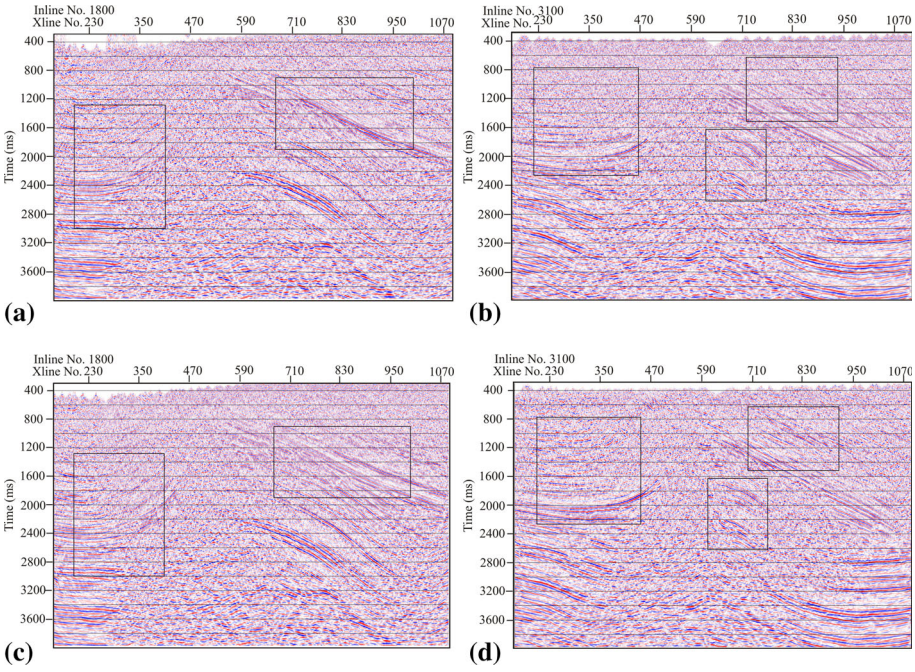

Fig. 4 Comparision of the PSTM and the CDS migration result **a** inline 1800 with the PSTM method, **b** inline 3100 with the PSTM method, **c** inline 1800 with the CDS method and **d** inline 3100 with the CDS method

common diffraction surface method. In comparing both results, it should be mentioned that the CDS processing approach yields a stacked solution that is subsequently time-migrated. Rectangles on the sections show places where new imaging method improved quality of the seismic image. Defining layer boundaries above the fault plane is not a difficult task in these sections. However, it is not easy to trace layer boundaries below the fault plane, due to the strong seismic energy attenuation. Therefore, according to the conceptual model, the faulted part could be traced to complete the stratigraphic interpretation. The final geologic model is shown in Fig. 5b that is in accordance with previous geological model obtained by Verges et al. (2011) shown in Fig. 5a.

5 The Pazanan area 3D seismic structural interpretation

Tamimi et al. (2009) stated that the Gachsaran Formation consisting of evaporites (anhydrite and salt) governs velocity of the seismic wave propagation in the media. Barzgar et al. (2015) demonestrated that seismic velocity of the Gachsaran Formation is affected by its predominant lithology and will increase by increasing amount of anhydrite. Therefore, the Gachsaran ridges show anomalous velocity behavior (Sherkati et al. 2006). Structural interpretation in this data was based on previous study of Abdollahie fard et al. (2011).

Lateral velocity changes and thick evaporite layer of the Gachsaran formation would distort time-migrated seismic sections obtained by the Kirchhoff algorithm. In this case, the Dix's hyperbolic moveout assumption is no longer valid and the stacked section is not a

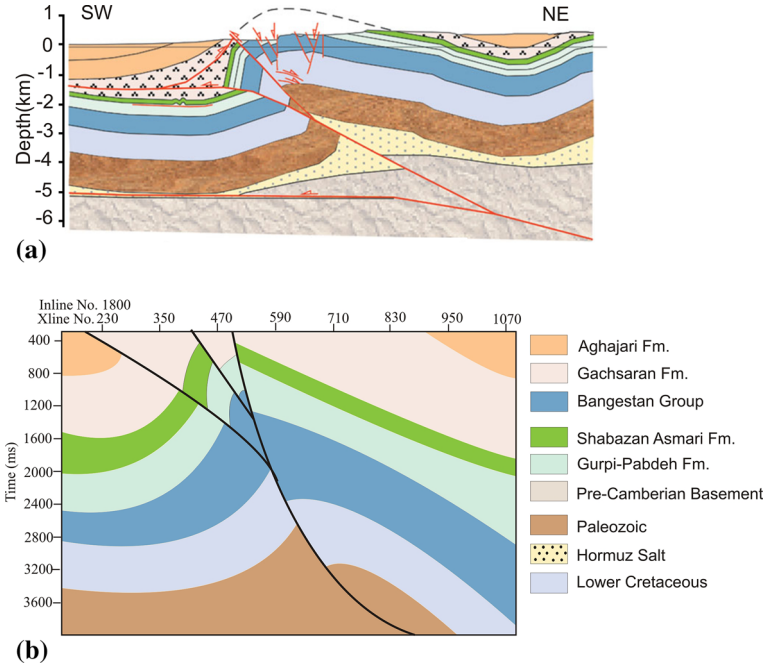

Fig. 5 **a** geological model from part of a Dezful Embayment (Verges et al. 2011) and **b** proposed geological cross section obtained from interpretation of seismic section shown in Fig. 4d

zero-offset section (Lambaré et al. 2007). Due to 3D nature of geological bodies and complicated geometry of seismic wave propagaton in the media, conventional 2D seismic processing techniques are unable to image geological bodies. (Cameron et al. 2008). In such a complicated case, 3D seismic imaging is needed to avoid interference of side effects and better focusing of seismic energy. Strong velocity change also make distortion on seismic image which could be resolved by building accurate velocity model and performing depth migration (Alaei 2006). The velocity model used here was obtained by the

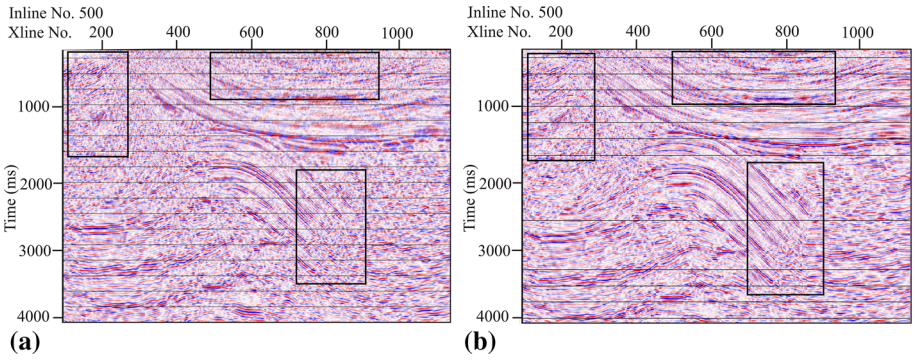

Fig. 6 An in-line from the 3D seismic data, **a** result of conventional PSTM and **b** result of 3D common diffraction surface method

method introduced by Adler et al. (2008). He introduced a nonlinear 3D tomographic least-square inversion of residual moveout in pre-stack-depth-migration common-image gathers.

Result of an inline of the 3D partial common diffraction method is shown in Fig. 6b, comparing with the result of conventional PSTM in Fig. 6a. Rectangles on both sections show improvement in seismic image quality by the proposed method compared to the PSTM method. Faults, anticline and different horizons are better identified in the up thrown side of the fault in Fig. 6b, while in the down thrown side; they only could be traced by the similarity in sequence of the layers obtained from the high quality part of the section.

As it could be seen in Fig. 6a, there is high elevation difference in both sides of the overthrust. There are also frequent small fault in top of the anticline that makes it difficult for an appropriate seismic imaging, in case of introducing strong velocity changes. The apparent detail of the fault traces in Fig. 6b, imply resolution greater than what was expected by the seismic coverage and Kirchhoff migration method, which proves ability of applying the 3D partial common diffraction surface method to provide enhanced seismic data for final depth imaging. The proposed structure of this area, based on interpretation of this section is shown in Fig. 7b, which is accordance with the geological model of the region obtained previously by Verges et al. (2011) shown in Fig. 7a. Structural interpretation in this data was in accordance with previous study of Chehri et al. (2014).

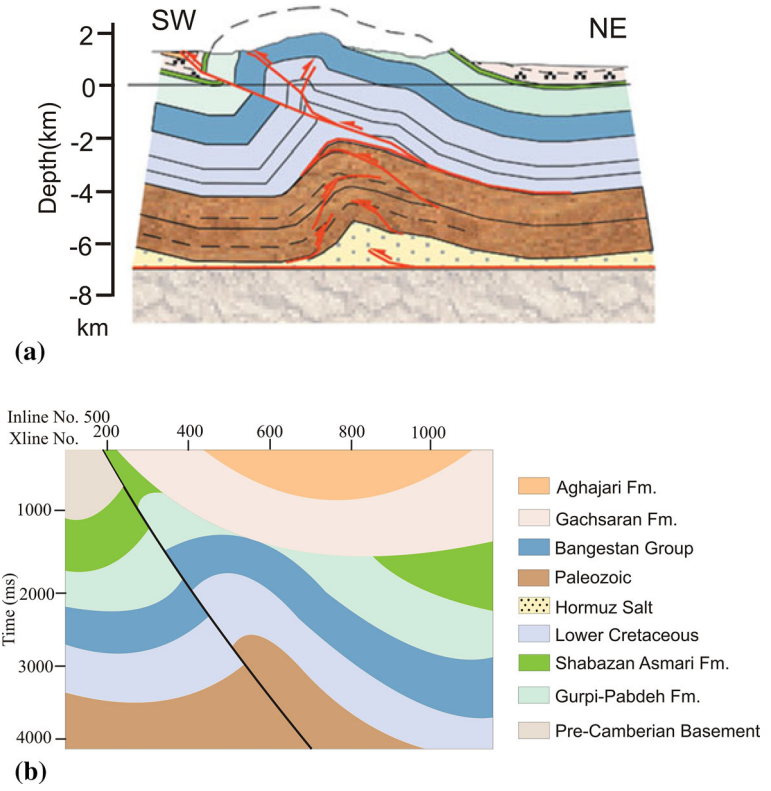

Fig. 7 **a** Geological model from part of a study area (Verges et al. 2011) and **b** proposed geological cross section obtained from interpretation of seismic section shown in Fig. 6b

Another inline from the Pazanan area is shown in Fig. 8. Like as the previous example of this area, the signal to noise ratio in seismic section obtained by the 3D partial diffraction is improved. Continuity of reflectors, location of faults and boundary of the anhydrite layers is better shown in Fig. 8b, compared to the prestack depth migration (PSDM) result in Fig. 8a. Rectangles in both sections, shows places of enhancement by the partial CDS method. The conceptual kinematic scenario for folding in the central Zagros is shown in Fig. 9a (Abdollahie Fard et al. 2011). The conceptual model, Fig. 9a(I), shows position of layers before deformation stage. Figure 9a(II) illustrates buckling and migration steps of the basal ductile unit toward the core of the detachment fold. Figure 9(III), shows development of folding and major thrust fault in deeper horizons and Fig. 9a(IV) is the present geoloical model (Abdollahie Fard et al. 2011). The proposed structure of this area based on interpretation of the section in Fig. 8d is illustrated in Fig. 9b.

6 The Izeh zone structural interpretation

Different studies showed that deformation system of the Izeh fault can't be recognizing only based on the geological field observation (Abdollahie Fard et al. 2006). To see whether the problems addressed above could be solved by imaging seismic data with the proposed method, a seismic data from the Izeh zone was selected for processing. In the first step, data was processed with the conventional PSTM method with the Kirchhoff algorithm, after applying pre-processing on the data. Figure 10a shows result of the conventional PSTM and Fig. 10b shows result of the 2D partial common diffraction surface imaging. As it could be seen, at the upper part of the section at small travel times, there is the Gachsaran formation depicts the folding system. Rectangles in both sections show parts of the data improved by the proposed method. The seismic section was interpreted according to the folding scenario for the Izeh zone (Sherkati and Letouzey 2004). Result of interpretation is shown in Fig. 11.

Figure 12 also shows another example from an oil field in the same region. The kinematic folding scenario shown in Fig. 12 and obtained from seismic sections in the Izeh region, was in good accordance with previous geological studies (Verges et al. 2011). In the seismic section, footwall synclines, low angle thrust faults, limb rotation and reduction in Gachsaran thickness during fold evolution are the specific characters of folds in the Izeh zone obtained by interpreting the enhanced seismic section.

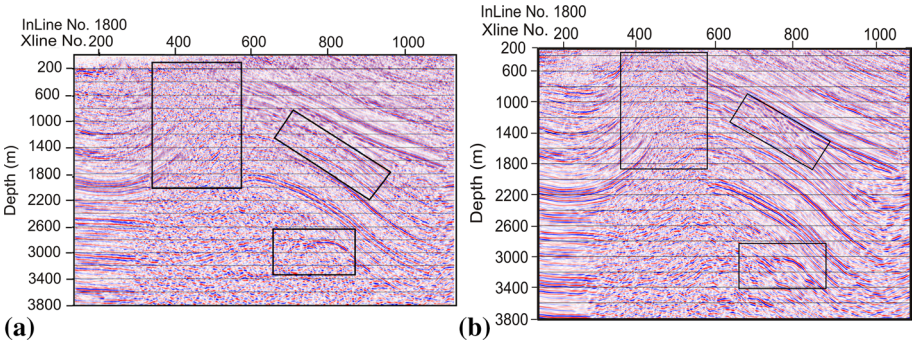

Fig. 8 Migrated section of in-line number 1800. **a** Result of conventional PSDM and **b** result of the 3D depth migration of partially enhanced pre-stack data

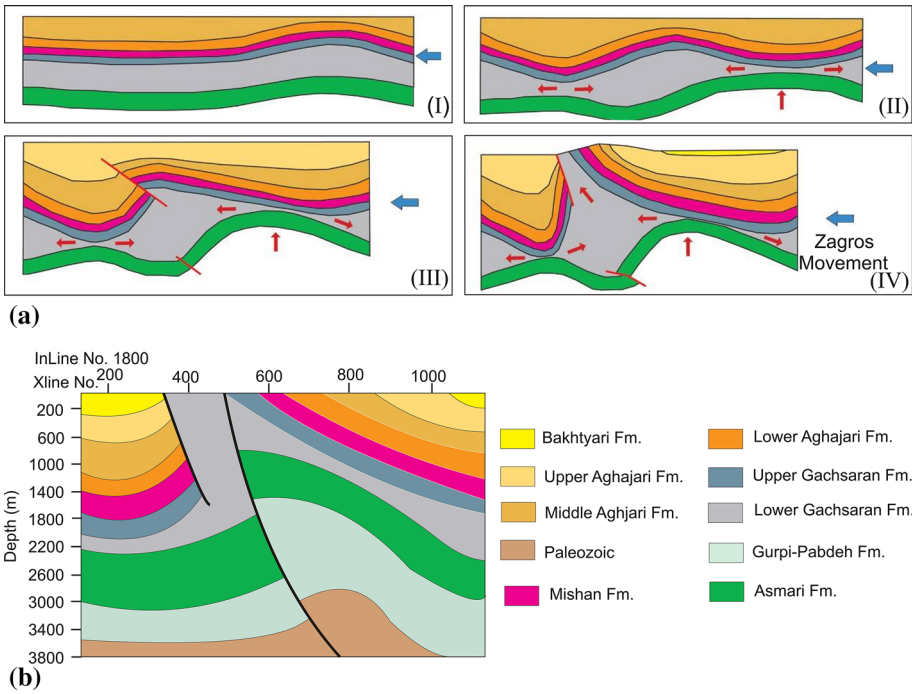

Fig. 9 **a** Geological evolution model from part of a study area (Abdollahie Fard et al. 2011). **b** Proposed geological cross section obtained from interpretation of seismic section shown in Fig. 8b

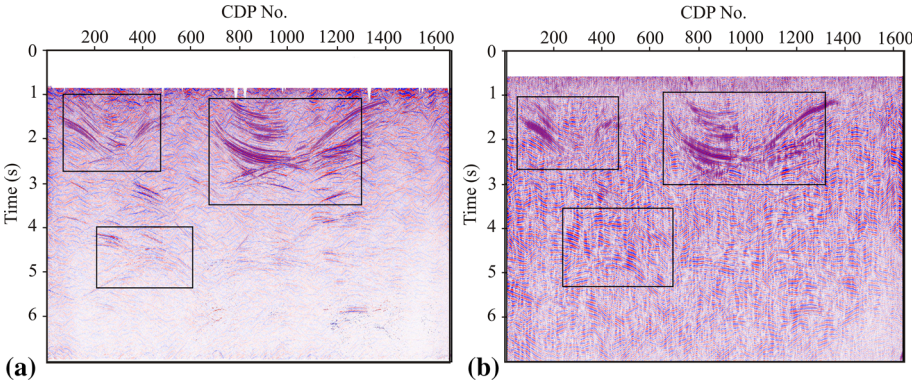

Fig. 10 The seismic section of the Izeh region obtained by **a** the conventional PSTM method and **b** the partial common diffraction surface method

7 The high Zagros zone seismic structural interpretation

The proposed seismic imaging procedure has been applied to a real dataset from the mountainous area of the high Zagros thrust fold belt of southwest Iran. In such complex geological settings, pre-stack depth imaging is the state-of-the-art solution but it is difficult to perform due to strong lateral seismic velocity change and difficult ray tracing or wave

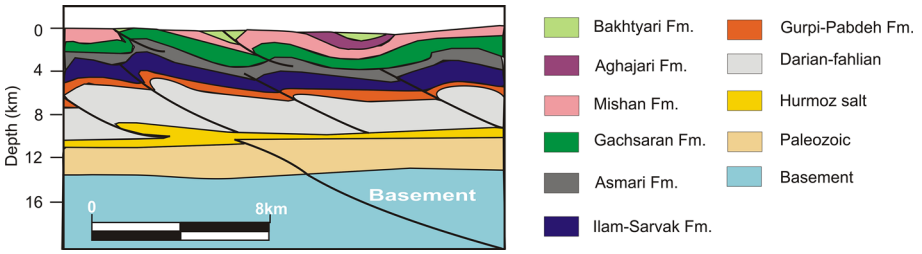

Fig. 11 The general folding in the Izeh region and interpretation of the seismic data based on interpretation of Fig. 10b

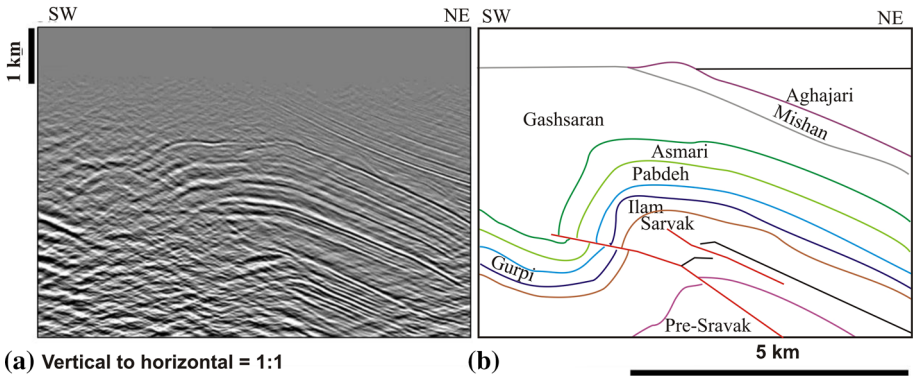

Fig. 12 Another seismic data with structural interpretation from the same region. **a** The seismic section, **b** the interpreted section showing horizons picked from the seismic section (modified after Abdolahie Fard et al. 2011)

propagation modeling (Zhu et al. 2014). Using imprecise velocity model for pre-stack depth migration can result in artifacts such as a poor focusing and vague positioning of reflectors in depth image (Robein 2010). To see whether the proposed method could resolve some of ambiguities in depth image, the 2D partial diffraction surface method was applied on a seismic data from high Zagros area. Seismic velocity is increasing rapidly with depth in this region and thus, velocity saturation occurs for larger traveltimes. Therefore, velocity search range in the 2D partial common diffraction surface method has to be determined sufficiently large in order not to lose reflection events in depth imaging procedure. Size of the aperture in midpoint direction was selected equal to 1300 *m*, to be close enough to the Fresnel zone size and also to increase the signal-to-noise ratio and continuity of events. The 2D partial diffraction surface section is shown in Fig. 13. As can be seen in Fig. 13b, quality of the migrated 2D partial common diffraction surface section is higher than the conventional PSTM result by the Kirchhoff algorithm shown in Fig. 13a. In the 2D partial diffraction surface section, more events could be seen and continuity of events is better preserved. Some of ambiguities that were visible in the PSTM section are resolved here by the 2D partial diffraction surface method. Circles in both sections show location where the proposed method could improve quality of the seismic image. Folding system especially in the upper left part of the section appears much clearer. Below the outstanding syncline, another folding is visible that is also not very clear in the PSTM section. In the 2D partial common diffraction surface section, anticline completely appears

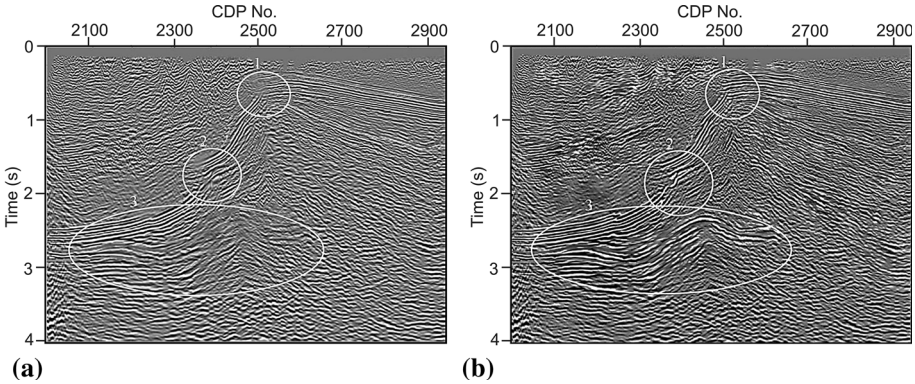

Fig. 13 Seismic section of the high Zagros region obtained by **a** the conventional PSTM method and **b** migration of the partial common diffraction surface stacked data

at large traveltimes. In the left part of the section, dipping layers are present that can hardly be seen in the PSTM section. Besides all these improvements, we can conclude that the 2D partial diffraction surface method could partially resolve the problem of imaging in complex structures. Structural interpretation in this data was based on the previous study of Letouzey and Sherkati (2003).

In the conceptual model with intermediate incompetent layer, phases *a* and *d* in Fig. 14, show state before deformation; without and with incompetent layer (here the Gachsaran Formation) respectively. Phases *b* and *e* depict buckling of the sedimentary pile and slip along the basal incompetent layer, without and with incompetent layer, respectively. In the presence of incompetent layers, the propagated fault dies out in the incompetent layer,

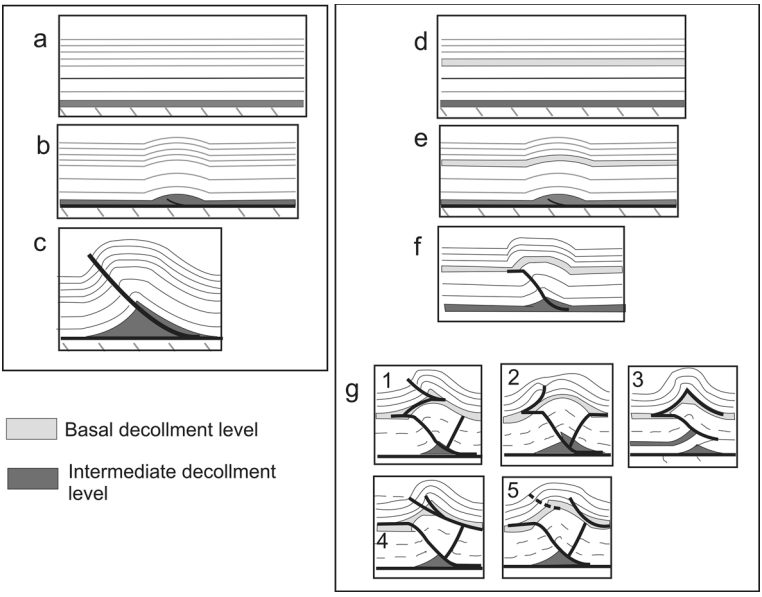

Fig. 14 The Conceptual kinematic scenario for folding in high Zagros obtained from seismic section in Fig. 13b and kinematic scenario introduced by Letouzey and Sherkati (2003)

(phase *f*) while a normal anticline is produced in the upper layer, and fault does not reach the surface.

Phase *g* illustrates development of secondary structures such as ''fishtail'' (g1 and g3) or ''rabbit ears'' folds (g2). The excess of shortening in the upper levels is transferred to an adjacent structure (g4 and g5). Based on this conceptual model, interpretation of the seismic section in Fig. 13b, was in accordance with previous presented kinematic scenario in this field (Letouzey and Sherkati 2003).

Saura et al. (2013) stated that in the Zagros area build-ups on top of anticlines recorded its growth and can be used as a dating method. General structural transects and balanced restoration of the central ZFTB in the area east of the Izeh zone and the Dezful Embayment is shown in Fig. 15 (Sherkati and Letouzey 2004). HZF, MFF and KMF in Fig. 15 are abbreviations of High Zagros fault, Mountain front fault and Kharg–Mish fault, respectively. Three small sections below the general model shows geological model obtained in this study from three different regions of the ZFTB. These three subsections are in good accordance with the general structural model of the ZFTB.

8 Conclusion

The pragmatic approach of Jäger et al. (2001) and the extended search strategy of Mann (2002) in the CRS stack method, have been combined with the concepts of dip move-out correction to completely resolve the problem of conflicting dips situation in complex geological structures seismic imaging. This improvement resulted in introduction of the CDS method and proposing this method for imaging in complex media (Soleimani 2015).

The CDS method focuses more on diffraction events and enhances diffractions compared to reflection events. To better solve the problem of imaging in complex structures,

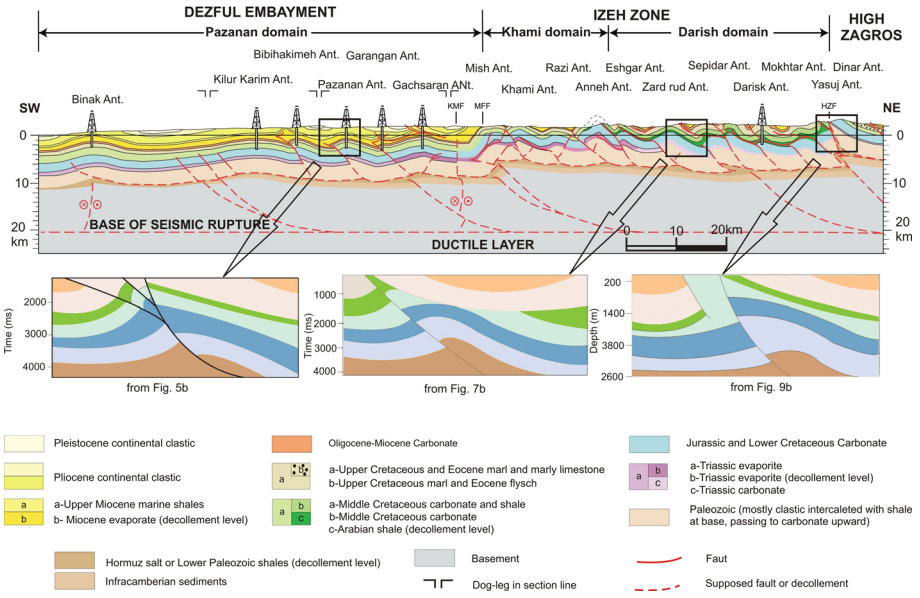

Fig. 15 (*Top*) Structural transects and balanced restoration of the central ZFTB (Sherkati and Letouzey 2004) and (*middle*) three geological model obtained in this study

the idea of Baykulov et al. (2011), that introduced the 2D partial CRS method, were combined by the 2D CDS method and resulted in introduction of the 2D partial common diffraction surface method here. In the other hand, the 2D partial common diffraction surface method was improved to 3D in this study. To see the ability of these methods in solving problem of imaging in complex structures, these methods were applied on real land seismic data from different regions of the Zagros thrust fault belt (ZTFB) of SW Iran. The structural analysis of the Pazanan oil field was performed on several seismic sections obtained by the new method. Layer boundaries were clearly identified in the new imaged section. Below the fault plane in the sections, the seismic energy attenuation due to the strong absorption of the Gachsaran formation was responsible for poor seismic quality. Well data was also available that controls elevation of the top of the formation on seismic section and controls accuracy of migration procedure. The structural analysis on sections shows that in the first stage of deformation, symmetric buckling of sedimentary rocks situated above the basal incompetent layer that is responsible for the first seed of folding. As deformation increased, the structures continue to buckle by hinge migration and limb rotation, which allowed folding to grow with transfer of material from synclines toward the anticlines. At this stage, thrust faults develop from deeper levels. Another 2D and 3D data used here were from the Izeh region selected for structural interpretation. The kinematic folding scenario from the Izeh region that was obtained by geological study was in good accordance with interpretation of the 2D and 3D seismic image obtained by the new proposed method. In the Izeh region, footwall synclines, low angle thrust faults, limb rotation and reduction in Gachsaran thickness during fold evolution were extracted from interpretation of the seismic sections from 2D partial diffraction surface method. Result of applying the improved strategy on real data from high Zagros, demonstrated that this strategy could completely overcome the problem of conflicting dips situations and yields a seismic section with more continuous events and more clear images of (previously obscured) weak events. Results of migration of a real data also showed that the migrated section of the partial common diffraction surface method is a suitable input for further structural interpretation. The new operator collects more energy that might not be stacked in the previous strategies. This leads to an improved image quality especially at discontinuities of the reflectors and in faulted parts of the section and also enhance diffraction events which improves the migration result. In the Dezful Embayment, the Gachsaran Formation decouples the folding above it from the folding below. It makes seismic imaging of potential traps beneath the detachment horizons extremely difficult which was resolved here by introducing and application of the partial common diffraction surface method.

References

Abdollahie Fard I, Braathen A, Mokhtari M, Alavi A (2006) Interaction of the Zagros Fold–Thrust Belt and the Arabian-type, deep-seated folds in the Abadan Plain and the Dezful Embayment, SW Iran. Pet Geosci 12:347–362

Abdollahie Fard I, Sepehr M, Sherkati S (2011) Neogene salt in SW Iran and its interaction with Zagros folding. Geol Mag 148(5–6):854–867

Adler F, Baina R, Soudani MA, Cardon P, Richard JB (2008) Nonlinear 3D tomographic least-squares inversion of residual moveout in Kirchhoff prestack-depth-migration common-image gathers. Geophysics 73(5):13–23

Alaei B (2005) Seismic forward modeling of two fault related folds from the Dezful Embayment of the Iranian Zagros mountaons. J Seism Explor 14:13–30

Alaei B (2006) An integrated procedure for migration velocity analysis in complex structures of thrust belts. J Appl Geophys 59:89–105
Albertin U, Woodward M, Kapoor J, Chang W, Charles S, Nichols D, Kitchenside P, Mao W (2001) Depth imaging example and methodology in the Gulf of Mexico. Lead Edge 20:498–513
Alen M, Talebian M (2011) Structural variation along the Zagros and the nature of the Dezful Embayment. Geol Mag 148(5–6):911–924
Barzgar E, Abdollahie Fard I, Moghaddam RH, Khalili EA, Garavan A (2015) Geological analysis and updating velocity model by restoration of a cross section in Zagros fold–thrust belt in the southwest of Iran. Arab J Geosci 8(10):8687–8702. doi:10.1007/s12517-015-1803-x
Baykulov M (2009) Seismic imaging in complex media with the Common Reflection Surface stack. Ph.D. thesis, Hamburg University
Baykulov M, Gajewski D (2009) Prestack seismic data enhancement with partial common-reflection-surface (CRS) stack. Geophysics 74:49–58
Baykulov M, Dummong S, Gajewski D (2011) From time to depth with CRS attributes. Geophysics 76:151–155
Berberian M, King GCP (1981) Towards a paleogeography and tectonic evolution of Iran. Can J Earth Sci 18:210–285
Biondi B (2006) 3D seismic imaging. Investigations in geophysics, 14, society of exploration geophysicists. SEG Publishing, Tulsa
Burberry CM, Cosgrove JW, Liu JG (2010) A study of fold characteristics and deformation style using the evolution of the land surface: Zagros Simply Folded Belt, Iran. Earth and Atmospheric Sciences. Paper 295
Cameron M, Fomel S, Sethian J (2008) Time-to-depth conversion and seismic velocity estimation using time-migration velocity. Geophysics 73:205–210
Chehri A, Kendall C, Ghadimvand NK, Samadi L (2014) Testing the controls on the seismic sequence stratigraphy of the Eocene–Oligocene boundary in Southern Iran with a Wheeler diagram derived from outcrops, seismic and well logs data. J Afr Earth Sci 100:324–334
Fomel S (2007) Velocity independent time domain seismic imaging using local event slopes. Geophysics 72(3):139–147
Gabtni H, Alyahyaoui S, Jallouli C, Hansi W, Mickous KL (2012) Gravity and seismic reflection imaging of a deep aquifer in an arid region: case history from the Jeffara basin, southeastern Tunisia. J Afr Earth Sci 66–67(15):85–97
Garabito G, Cruz JCR, Söllner W (2009). Macro-model independent migration to zero offset (CRS-MZO). In: 11th international congress of the Brazilian Geophysical Society and EXPOGEF, Salvador, Bahia, pp 1513–1516. doi:10.1190/sbgf2009-320
Gelchinsky B, Berkovitch A, Keydar S (1999) Multifocussing homeomorphic imaging: part 1. Basic concepts and formulas. J Appl Geophys 42:229–242
Gjøystdal H, Iversen E, Lecomte I, Kaschwich T, Drottning A, Mispel J (2007) Improved applicability of ray tracing in seismic acquisition, imaging, and interpretation. Geophysics 75:261–271
Höcht G, de Bazelaire E, Majer P, Hubral P (1999) Seismic and optics: hyperbolae and curvatures. J Appl Geophys 42:261–281
Huang Y, Lin D, Bai B, Roby S, Ricardez C (2010) Challenges in pre-salt depth imaging of the deep water Santos Basin, Brazil. Lead Edge 29:820–825
Jäger R (1999) The common reflection surface stack: theory and application. Diploma thesis, University of Karlsruhe
Jäger R, Mann J, Höcht G, Hubral P (2001) Common reflection surface stack: image and attributes. Geophysics 66:97–109
Lambaré G, Herrmann P, Guillaume P, Zimine S, Wolfarth S, Hermant O, Butt S (2007) From time to depth imaging with Beyond Dix. First Break 25:71–76
Letouzey J, Sherkati S (2003) Movement, tectonic events and structural style, in the central Zagros fold and thrust belt (Iran). AAPG annual meeting (abstract)
Letouzey J, Sherkati S, Mengus JM, Motiei H, Ehsani M, Ahmadnia A, Rudkiewicz JL (2002) A regional structural interpretation of the Zagros Mountain Belt in Northern Fars and High Zagros (SW Iran). AAPG annual meeting
Lu Z, Gao R, Li Q, He R, Kuang C, Hou H, Xiong X, Guan Y, Wang H, Klemperer SL (2009) Test of deep seismic reflection profiling across central uplift of Qiangtang terrane in Tibetan plateau. J Earth Sci 20(2):438–447
Mann J (2002) Extensions and applications of the common-reflection-surface stack method: Ph.D. thesis, University of Karlsruhe

Mann J, Jäger R, Müller T, Höcht G, Hubral P (1999) Common-reflection-surface stack: a real data example. J Appl Geophys 42(3–4):301–318. doi:10.1016/S0926-9851(99)00042-7
Müller T (1999) The common reflection surface stack method—seismic imaging without explicit knowledge of the velocity model. Ph.D. thesis, University of Karlsruhe, Germany
Müller A (2003) The 3D common-surface-reflection stack-theory and application. Master thesis, University of Karlsruhe
Olabode SO, Adekoya JA (2008) Seismic stratigraphy and development of Avon canyon in Benin (Dahomey) basin, southwestern Nigeria. J Afr Earth Sci 50(5):286–304
Pu R, Zhu L, Zhong H (2009) 3-D seismic identification and characterization of ancient channel morphology. J Earth Sci 20(5):858–867
Pu R, Zhang Y, Luo J (2012) Seismic reflection, distribution, and potential trap of Permian volcanic rocks in the Tahe field. J Earth Sci 23(4):421–430
Pu R, Yun L, Su J, Guo Q, Dang X (2014) Growth conditions and 3-D seismic delineation of carboniferous barrier reefs in the southwestern Tarim Basin. J Earth Sci 25(2):315–323
Raef A (2009) Land 3D-seismic data: preprocessing quality control utilizing survey design specifications, noise properties, normal moveout, first breaks, and offset. J Earth Sci 20(3):640–648
Ray A, Pfau G, Chen R (2004) Importance of ray trace modeling in the discovery of the Thunder Horse North Filed, Gulf of Mexico. Lead Edge 23:68–70
Robein E (2010) Seismic imaging. European Association of Geoscientists and Engineers, (EAGE) publication, Netherlands
Saura E, Embry JC, Vergés J, Hunt DW, Casciello E, Homke S (2013) Growth fold controls on carbonate distribution in mixed foreland basins: insights from the Amiran foreland basin (NW Zagros, Iran) and stratigraphic numerical modelling. Basin Res 25:149–171
Seitchick A, Jurick D, Bridge A, Brietzke R, Beeney K, Codd J, Hoxha F, Pignol C, Kessler D (2009) The Tempest Project addressing challenges in deep water Gulf of Mexico depth imaging through geologic models and numerical simulation. Lead Edge 28:546–553
Sepehr M, Cosgrove JW (2004) Structural framework of the Zagros Fold–Thrust Belt, Iran. Mar Pet Geol 21:829–843
Sepehr M, Corgrove J, Moeini M (2006) The impact of cover rock rheology on the style of folding in the Zagros fold-thrust belt. Techtonophysics 427(1–4):265–281. doi:10.1016/j.tecto.2006.05.021
Sherkati S, Letouzey J (2004) Variation of structural style and basin evolution in the central Zagros (Izeh zone and Dezful Embayment), Iran. Mar Pet Geol 21:535–554
Sherkati S, Molinaro M, Frizon de Lamotte D, Letouzey J (2005) Detachment folding in the central and eastern Zagros fold-belt (Iran). J Struct Geol 27:1680–1696
Sherkati S, Letouzey J, Frizon de Lamotte D (2006) Central Zagros fold-thrust belt (Iran): new insights from seismic data, field observation, and sandbox modeling. Tectonics 25(4):1–27. doi:10.1029/2004TC001766
Soleimani M (2015) Seismic imaging of mud volcano boundary in the east of Caspian Sea by common diffraction surface stack method. Arab J Geosci 8(6):3943–3958. doi:10.1007/s12517-014-1497-5
Soleimani M, Mann J (2008) Merging aspects of DMO correction and CRS stack to account for conflicting dips situations. Annual WIT report, pp 159–166
Soleimani M, Piruz I, Mann J, Hubral P (2009) Common reflection surface stack; accounting for conflicting dips situations by considering all possible dips. J Seism Explor 18:271–288
Tamimi N, Abdoallhie Frad I, Sherkati S (2009) The effects of structural components on seismic wave velocity in incompetent units, case study: Gachsaran Formation, SW Iran. SEG annual meeting, Houston, Texas. SEG-2009-3750
Verges J, Saura E, Casciello E, Fernandez M, Villasenor A, Jimenez-munt I, Garcia-Castellanos D (2011) Crustal-scale cross-sections across the NW Zagros belt: implications for the Arabian margin reconstruction. Geol Mag 148(5–6):739–761
Wang K, Luo Y, Zaho K, Zhang L (2014) Body waves revealed by spatial stacking on long-term cross-correlation of ambient noise. J Earth Sci 25(6):977–984
Xu B, Xiao A, Wu L, Mao L, Dong Y, Zhou L (2014) 3D seismic attributes for structural analysis in compressional context: a case study from western Sichuan Basin. J Earth Sci 25(6):985–990
Zhu X, Gao R, Li Q, Guan Y, Lu Z, Wang H (2014) Static corrections methods in the processing of deep reflection seismic data. J Earth Sci 25(2):299–308